

Final results of $\bar{\nu}_e - e$ scattering cross-section measurements and constraints on new physics

Muhammed Deniz ^{a,b,c}, Selcuk Bilmis ^{b,c} and Henry T. Wong ^c
(on behalf of the TEXONO Collaboration)

^a Department of Physics, Karadeniz Technical University, Trabzon 61080, Turkey.

^b Department of Physics, Middle East Technical University, Ankara 06531, Turkey.

^c Institute of Physics, Academia Sinica, Taipei 11529, Taiwan.

E-mail: htwong@phys.sinica.edu.tw

Abstract.

The $\bar{\nu}_e - e$ elastic scattering cross-section was measured with a CsI(Tl) scintillating crystal detector array with a total mass of 187 kg at the Kuo-Sheng Nuclear Power Station. The detectors were exposed to a reactor $\bar{\nu}_e$ flux of $6.4 \times 10^{12} \text{ cm}^{-2} \text{ s}^{-1}$ originated from a core with 2.9 GW thermal power. Using 29882/7369 kg-days of Reactor ON/OFF data, the Standard Model (SM) of electroweak interaction was probed at the 4-momentum transfer range of $Q^2 \sim 3 \times 10^{-6} \text{ GeV}^2$. A cross-section ratio of $R_{\text{expt}} = [1.08 \pm 0.21 \text{ (stat)} \pm 0.16 \text{ (sys)}] \times R_{\text{SM}}$ was measured. Constraints on the electroweak parameters (g_V, g_A) were placed, corresponding to a weak mixing angle measurement of $\sin^2 \theta_W = 0.251 \pm 0.031 \text{ (stat)} \pm 0.024 \text{ (sys)}$. Destructive interference in the SM $\bar{\nu}_e - e$ processes was verified. Bounds on neutrino anomalous electromagnetic properties (neutrino magnetic moment and neutrino charge radius), non-standard neutrino interactions, upparticle physics and non-commutative physics were placed. We summarize the experimental details and results, and discuss projected sensitivities with realistic and feasible hardware upgrades.

Neutrino-electron scattering is pure leptonic process which is exactly evaluated with electroweak theory. Cross-section measurement of $\bar{\nu}_e - e$ scattering with reactor neutrinos [1] provides a new window to study the Standard Model (SM) electroweak parameters as well as anomalous neutrino electromagnetic properties such as charge radius and magnetic moments in a different kinematics regime from that at accelerator. In addition, new physics beyond SM such as Non-Standard neutrinos interaction (NSI) and Unparticle Physics (UP) [2], as well as the scale (Λ_{NC}) for Non-commutative Physics [3] can be probed. The $\bar{\nu}_e - e$ scattering cross-section in the laboratory frame is:

$$\left[\frac{d\sigma}{dT}(\bar{\nu}_e e) \right]_{SM} = \frac{G_F^2 m_e}{2\pi} \cdot [(g_V - g_A)^2 + (g_V + g_A + 2)^2 \left(1 - \frac{T}{E_\nu} \right)^2 - (g_V - g_A)(g_V + g_A + 2) \frac{m_e T}{E_\nu^2}], \quad (1)$$

where G_F is the Fermi constant, T is the kinetic energy of the recoil electron, E_ν is the incident neutrino energy, m_e is mass of the electron and g_V, g_A are, respectively, the vector and axial-vector coupling constants. The SM assignments to the coupling constants are: $g_V = -\frac{1}{2} + 2 \sin^2 \theta_W$ and $g_A = -\frac{1}{2}$, where $\sin^2 \theta_W$ is the weak mixing angle. Interactions of $\bar{\nu}_e - e$ and $\nu - e$ are two of the few SM processes which proceed via charged- and neutral-currents *and* their interference, such that the event rates (R) can be expressed by its components as: $R_{\text{expt}} = R_{CC} + R_{NC} + \eta \cdot R_{Int}$.

A model-independent formulation of NSI is to characterize $\nu - e$ scatterings as four-Fermi interactions with new couplings $\varepsilon_{\alpha\beta}^{eP}$ which describe the coupling strength with respect to G_F . The

helicity states are denoted by P (=L,R), and (α, β) stand for the lepton flavor (e, μ or τ) for the incoming/outgoing neutrinos. The cases where $\alpha = \beta$ and $\alpha \neq \beta$ correspond to Non-Universal (NU) and Flavor-Changing (FC) NSI, respectively. The $\bar{\nu}_e - e$ cross-section including both SM and NSI is given by [4]:

$$\left[\frac{d\sigma}{dT} \right]_{SM+NSI} = \frac{2G_F^2 m_e}{\pi} \cdot \left[\left(\tilde{g}_R^2 + \sum_{\alpha \neq e} |\epsilon_{\alpha e}^{eR}|^2 \right) + \left((\tilde{g}_L + 1)^2 + \sum_{\alpha \neq e} |\epsilon_{\alpha e}^{eL}|^2 \right) \left(1 - \frac{T}{E_V} \right)^2 - \left(\tilde{g}_R (\tilde{g}_L + 1) + \sum_{\alpha \neq e} |\epsilon_{\alpha e}^{eR}| |\epsilon_{\alpha e}^{eL}| \right) \frac{m_e T}{E_V^2} \right], \quad (2)$$

where $\tilde{g}_L = g_L + \epsilon_{ee}^{eL}$ and $\tilde{g}_R = g_R + \epsilon_{ee}^{eR}$, defined in terms of the chiral couplings: $g_L = \frac{1}{2}(g_V + g_A) = -\frac{1}{2} + \sin^2 \theta_W$ and $g_R = \frac{1}{2}(g_V - g_A) = \sin^2 \theta_W$.

The measurement of $\bar{\nu}_e - e$ elastic scattering at $Q^2 \sim \text{MeV}^2$ was performed by the TEXONO Collaboration at the Kuo-Sheng Reactor Neutrino Laboratory in Taiwan. The experimental details were documented in Refs. [1, 5]. The CsI(Tl) target crystals were configured as a 12×9 array inside a shielding structure with ~ 50 tons of materials enclosed by an active cosmic-ray scintillator veto (CRV) system. Each single crystal module has a hexagonal-shaped cross-section with 2 cm side, 40 cm length and modular mass of 1.87 kg. The detector consisted of 100 crystals giving a total mass of 187 kg. The light output was read out at both ends of the crystal by photomultipliers (PMTs) with low-activity glass of 29 mm diameter. The PMT signals were recorded by 20 MHz Flash Analog-to-Digital-Converters (FADCs) running on a VME-based data acquisition system. The sum of the two PMT signals gives the energy of the event, while their difference provides information on the longitudinal ‘‘Z’’ position. An energy resolution of 4% and a Z-resolution of < 1 cm RMS at 660 keV as well as excellent α/γ event identification by pulse shape discrimination (PSD) were demonstrated.

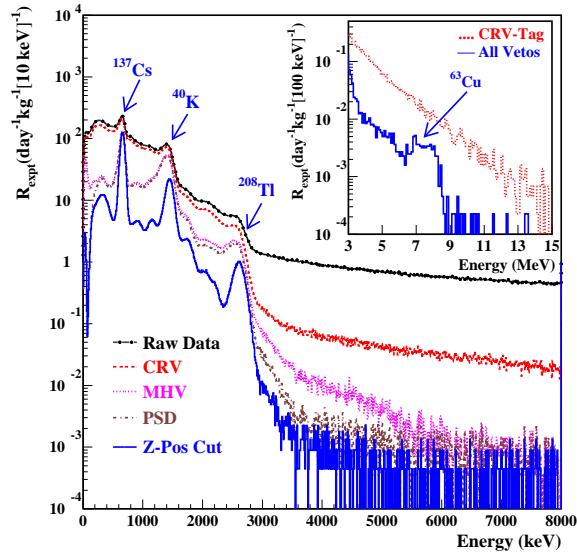


Figure 1. The measured energy spectra at various stages of the analysis showing the effects of successive selection cuts.

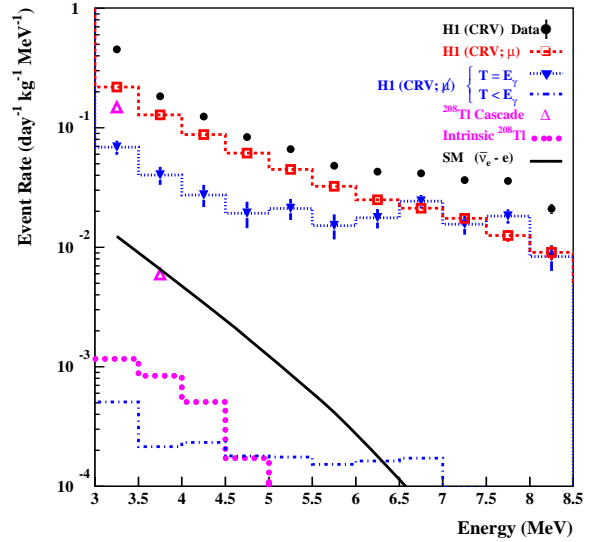


Figure 2. Measured H1 spectrum and the different evaluated background channels. The SM $\bar{\nu}_e - e$ contributions are overlaid.

Neutrino-induced candidate ‘‘single-hit (H1)’’ events were selected through the event-by-event suppression in the various background channels: (a) cosmic-ray induced events by CRV, (b) γ -induced anti-Compton events by multiplicity veto (MHV), (c) accidental and α - events by PSD, and (c) external

background by longitudinal Z-position cut. Residual H1 background channels at the relevant 3–8 MeV range are depicted in Figure 2, where the dominant components include: (i) cosmic-ray induced events where CRV are missing; (ii) ambient high energy γ -rays following neutron capture of ^{63}Cu ; and (iii) cascade γ -rays from ^{208}Tl . Their contributions were evaluated from *in situ* measurement of CRV inefficiencies, multi-hit samples and the ^{208}Tl -2614 keV lines, coupled with simulation studies. and the results provide the second background measurement. The combined background (BKG) were statistically subtracted from the H1 spectra.

A total of 29882/7369 kg-day of Reactor ON/OFF data was recorded. The *OFF* – *BKG* spectrum is consistent with zero showing the background modeling and subtraction is valid. The combined *ON* – *BKG* residual spectrum is displayed in Figure 3, from which various electroweak parameters were derived. The excess in the residual spectrum corresponds to ~ 414 neutrino-induced events, and an event-rate relative to that of SM at a ratio of $\xi \equiv R_{\text{expt}}/R_{\text{SM}} = [1.08 \pm 0.21(\text{stat}) \pm 0.16(\text{sys})]$ which implies $\sin^2\theta_W = 0.251 \pm 0.031(\text{stat}) \pm 0.024(\text{sys})$. The allowed region in the $g_V - g_A$ plane is depicted in Figure 4. The accuracy improves over previous reactor $\bar{\nu}_e - e$ experiments [1] as well as that in accelerator-based $\nu_e - e$ scattering experiments [6]. The measured interference parameter of $\eta = -0.92 \pm 0.30(\text{stat}) \pm 0.24(\text{sys})$ verifies the SM prediction of destructive interference ($\eta_{\text{SM}} = -1$).

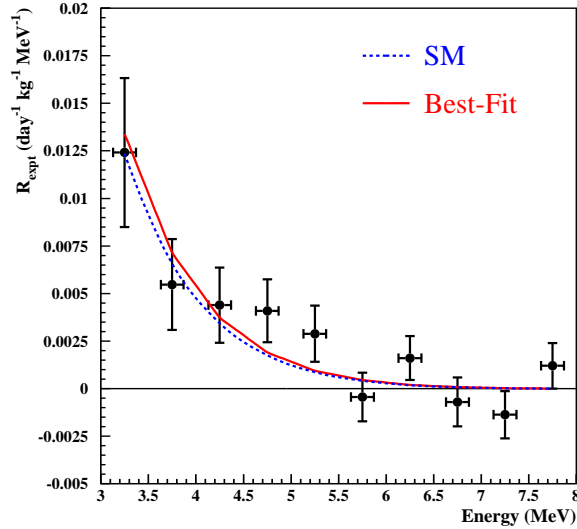


Figure 3. The combined ON-BKG residual spectrum together with those of SM and best-fit results.

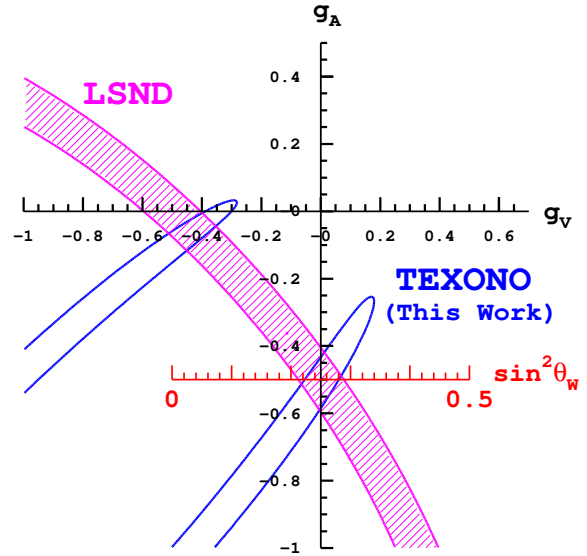


Figure 4. The 1σ allowed region in $g_V - g_A$ space, and in the $\sin^2\theta_W$ axis, for both $\bar{\nu}_e - e$ (TEXONO) and $\nu_e - e$ (LSND) scattering experiments.

Existence of neutrino magnetic moment ($\mu_{\bar{\nu}_e}$) would contribute an additional term to the cross-section of Eq. 1:

$$\left(\frac{d\sigma}{dT}\right)_{\mu_\nu} = \frac{\pi\alpha_{em}^2\mu_\nu^2}{m_e^2} \left[\frac{1 - T_e/E_\nu}{T_e} \right], \quad (3)$$

where α_{em} is the fine structure constant. From a best-fit analysis, a limit of $\mu_{\bar{\nu}_e} < 2.2 \times 10^{-10} \times \mu_B$ at 90% confidence level (CL) was derived. A finite neutrino charge radius $\langle r_{\bar{\nu}_e}^2 \rangle$ would lead to radiative corrections which modify the electroweak parameters by $g_V \rightarrow -\frac{1}{2} + 2\sin^2\theta_W + (2\sqrt{2}\pi\alpha_{em}/3G_F)\langle r_{\bar{\nu}_e}^2 \rangle$ and $\sin^2\theta_W \rightarrow \sin^2\theta_W + (\sqrt{2}\pi\alpha_{em}/3G_F)\langle r_{\bar{\nu}_e}^2 \rangle$. The allowed range at 90% CL is $-2.1 \times 10^{-32} < \langle r_{\bar{\nu}_e}^2 \rangle < 3.3 \times 10^{-32}$. New constraints on NSI and UP couplings [2] as well as on Λ_{NC} [3] were also derived, as displayed in Table 1 for those of NSI.

Table 1. Constraints at 90% CL on the NSI couplings. The projected sensitivities correspond to improved features listed in Table 2.

NSI		Measurement		Bounds	Projected
Parameters		Best-Fit \pm stat. \pm sys	χ^2/dof	at 90% C.L.	Sensitivities
NU {	$\epsilon_{ee}^{\text{eL}}$	$\epsilon_{ee}^{\text{eL}} = 0.03 \pm 0.26 \pm 0.17$	8.9/9	$-1.53 < \epsilon_{ee}^{\text{eL}} < 0.38$	± 0.015
	$\epsilon_{ee}^{\text{eR}}$	$\epsilon_{ee}^{\text{eR}} = 0.02 \pm 0.04 \pm 0.02$	8.7/9	$-0.07 < \epsilon_{ee}^{\text{eR}} < 0.08$	± 0.002
FC {	$\epsilon_{e\mu}^{\text{eL}}, \epsilon_{e\tau}^{\text{eL}}$	$\epsilon_{e\mu}^{\text{eL}2}(\epsilon_{e\tau}^{\text{eL}2}) = 0.05 \pm 0.27 \pm 0.24$	8.9/9	$ \epsilon_{e\mu}^{\text{eL}} (\epsilon_{e\tau}^{\text{eL}}) < 0.84$	± 0.052
	$\epsilon_{e\mu}^{\text{eR}}, \epsilon_{e\tau}^{\text{eR}}$	$\epsilon_{e\mu}^{\text{eR}2}(\epsilon_{e\tau}^{\text{eR}2}) = 0.008 \pm 0.015 \pm 0.012$	8.7/9	$ \epsilon_{e\mu}^{\text{eR}} (\epsilon_{e\tau}^{\text{eR}}) < 0.19$	± 0.007

Table 2. Projected statistical sensitivities on ξ and $\sin^2\theta_W$ under various realistically achievable improvement to the experiment.

Improvement	$\Delta_{stat}(\xi)$	$\Delta_{stat}[\sin^2\theta_W]$
This Work	0.21	0.031
Improved Feature :		
A. $\times 30$ Data Strength	0.038	0.0057
B. Background Reduction		
B1: $>99\%$ Cosmic-Ray Efficiency	0.12	0.018
B2: $\times \frac{1}{10}$ Reduction in Ambient & ^{208}Tl γ 's	0.16	0.024
* With Both B1+B2	0.05	0.007
All Features A+B1+B2 Combined	0.009	0.0013

The sensitivities can be further enhanced in future experiments. As illustrations, the projected improvement under various realistically achievable assumptions are summarized in Table 2. Electromagnetic calorimeters using CsI(Tl) with tens of tons of mass have been constructed, such that the target mass is easily expandable. As shown in Figure 2, the dominant background above 3 MeV were all external to the target scintillator. Accordingly, they will be attenuated effectively through self-shielding in a target with bigger mass. The incorporated features listed in Table 2 correspond to 30 times increase in data strength (for instance, with 1 ton fiducial mass and 1000 days data taking) and $\times 1/10$ suppression in background. The statistical accuracies can be improved to 0.8% and 0.12% for ξ and $\sin^2\theta_W$, respectively. Systematic uncertainties originate mainly from the evaluation of the reactor neutrino spectra. This can be overcome by a simultaneous measurement of the $\bar{\nu}_e$ spectra via the matured inverse beta-decay process $\bar{\nu}_e + p \rightarrow n + e^+$ with, for instance, large liquid scintillator detectors.

References

- [1] Deniz M et al. 2010 *Phys. Rev. D* **81** 072001, and references therein.
- [2] Deniz M et al. 2010 *Phys. Rev. D* **82** 033004, and references therein.
- [3] Bilmis S et al. 2012 *arXiv: 1201.3996 [hep-ph]*, and references therein.
- [4] Barranco J et al. 2006 *Phys. Rev. D* **73** 113001; Barranco J et al. 2008 *Phys. Rev. D* **77** 093014.
- [5] Wong H T et al. 2000 *Astroparticle Phys.* **14** 141; Li H B et al. 2001 *Nucl. Instrum. and Meth. A* **459** 93; Lai W P et al. 2001 *Nucl. Instrum. and Meth. A* **465** 550; Liu Y et al. 2002 *Nucl. Instrum. and Meth. A* **482** 125; Zhu Y F et al., 2006 *Nucl. Instr. and Meth. A* **557**, 490; Wong H T et al., 2007 *Phys. Rev. D* **75** 012001.
- [6] Allen R C et. al. 1993 *Phys. Rev. D* **47** 11; Aurbach L B et. al. 2001 *Phys. Rev. D* **63** 112001.